# Observation of discrete diffraction patterns in an optically induced lattice

**Jiteng Sheng,[1] Jing Wang,[1] Mohammad-Ali Miri,[2] Demetrios N. Christodoulides,[2] and Min Xiao[1,*]**

[1]*Department of Physics, University of Arkansas, Fayetteville, AR 72701, USA*
[2]*CREOL, College of Optics and Photonics, University of Central Florida, Orlando, Florida 32816, USA*
**mxiao@uark.edu*

**Abstract:** We have experimentally observed the discrete diffraction of light in a coherently prepared multi-level atomic medium. This is achieved by launching a probe beam into an optical lattice induced from the interference of two coupling beams. The diffraction pattern can be controlled through the atomic parameters such as two-photon detuning and temperature, as well as orientations of the coupling and probe beams. Clear diffraction patterns occur only near the two-photon resonance.

©2015 Optical Society of America

**OCIS codes:** (270.1670) Coherent optical effects; (050.1940) Diffraction; (190.4180) Multiphoton processes.

## References and links

1. D. N. Christodoulides, F. Lederer, and Y. Silberberg, "Discretizing light behaviour in linear and nonlinear waveguide lattices," Nature **424**(6950), 817–823 (2003).
2. I. L. Garanovich, S. Longhi, A. A. Sukhorukov, and Y. S. Kivshar, "Light propagation and localization in modulated photonic lattices and waveguides," Phys. Rep. **518**(1-2), 1–79 (2012).
3. R. Morandotti, U. Peschel, J. S. Aitchison, H. S. Eisenberg, and Y. Silberberg, "Experimental observation of linear and nonlinear optical Bloch oscillations," Phys. Rev. Lett. **83**(23), 4756–4759 (1999).
4. T. Pertsch, P. Dannberg, W. Elflein, A. Bräuer, and F. Lederer, "Optical Bloch oscillations in temperature tuned waveguide arrays," Phys. Rev. Lett. **83**(23), 4752–4755 (1999).
5. H. Trompeter, W. Krolikowski, D. N. Neshev, A. S. Desyatnikov, A. A. Sukhorukov, Y. S. Kivshar, T. Pertsch, U. Peschel, and F. Lederer, "Bloch oscillations and Zener tunneling in two-dimensional photonic lattices," Phys. Rev. Lett. **96**(5), 053903 (2006).
6. A. Peruzzo, M. Lobino, J. C. F. Matthews, N. Matsuda, A. Politi, K. Poulios, X. Q. Zhou, Y. Lahini, N. Ismail, K. Wörhoff, Y. Bromberg, Y. Silberberg, M. G. Thompson, and J. L. OBrien, "Quantum walks of correlated photons," Science **329**(5998), 1500–1503 (2010).
7. T. Schwartz, G. Bartal, S. Fishman, and M. Segev, "Transport and Anderson localization in disordered two-dimensional photonic lattices," Nature **446**(7131), 52–55 (2007).
8. Z. Chen and H. Martin, "Waveguides and waveguide arrays formed by incoherent light in photorefractive materials," Opt. Mater. **23**(1-2), 235–241 (2003).
9. J. W. Fleischer, M. Segev, N. K. Efremidis, and D. N. Christodoulides, "Observation of two-dimensional discrete solitons in optically induced nonlinear photonic lattices," Nature **422**(6928), 147–150 (2003).
10. N. K. Efremidis, S. Sears, D. N. Christodoulides, J. W. Fleischer, and M. Segev, "Discrete solitons in photorefractive optically induced photonic lattices," Phys. Rev. E Stat. Nonlin. Soft Matter Phys. **66**(4), 046602 (2002).
11. D. N. Neshev, T. J. Alexander, E. A. Ostrovskaya, Y. S. Kivshar, H. Martin, I. Makasyuk, and Z. Chen, "Observation of discrete vortex solitons in optically induced photonic lattices," Phys. Rev. Lett. **92**(12), 123903 (2004).
12. R. Kapoor and G. S. Agarwal, "Theory of electromagnetically induced waveguides," Phys. Rev. A **61**(5), 053818 (2000).
13. P. K. Vudyasetu, D. J. Starling, and J. C. Howell, "All optical waveguiding in a coherent atomic rubidium vapor," Phys. Rev. Lett. **102**(12), 123602 (2009).
14. A. G. Truscott, M. E. J. Friese, N. R. Heckenberg, and H. Rubinsztein-Dunlop, "Optically written waveguide in an atomic vapor," Phys. Rev. Lett. **82**(7), 1438–1441 (1999).
15. S. E. Harris, "Electromagnetically induced transparency," Phys. Today **50**(7), 36 (1997).
16. J. P. Marangos, "Electromagnetically induced transparency," J. Mod. Opt. **45**(3), 471–503 (1998).
17. J. Gea-Banacloche, Y. Li, S. Jin, and M. Xiao, "Electromagnetically induced transparency in ladder-type inhomogeneously broadened media: theory and experiment," Phys. Rev. A **51**(1), 576–584 (1995).
18. M. Xiao, Y. Li, S. Jin, and J. Gea-Banacloche, "Measurement of dispersive properties of electromagnetically induced transparency in rubidium atoms," Phys. Rev. Lett. **74**(5), 666–669 (1995).

#240649 Received 11 May 2015; revised 25 Jun 2015; accepted 28 Jun 2015; published 22 Jul 2015
© 2015 OSA

19. R. R. Moseley, S. Shepherd, D. J. Fulton, B. D. Sinclair, and M. H. Dunn, "Spatial consequences of electromagnetically induced transparency: observation of electromagnetically induced focusing," Phys. Rev. Lett. **74**(5), 670–673 (1995).
20. J. Wen, S. Du, H. Chen, and M. Xiao, "Electromagnetically induced Talbot effect," Appl. Phys. Lett. **98**(8), 081108 (2011).
21. H. Ling, Y. Li, and M. Xiao, "Electromagnetically induced grating: homogeneously broadened medium," Phys. Rev. A **57**(2), 1338–1344 (1998).
22. Z. H. Xiao, L. Zheng, and H. Lin, "Photoinduced diffraction grating in hybrid artificial molecule," Opt. Express **20**(2), 1219–1229 (2012).
23. M. Mitsunaga and N. Imoto, "Observation of an electromagnetically induced grating in cold sodium atoms," Phys. Rev. A **59**(6), 4773–4776 (1999).
24. G. C. Cardoso and J. W. Tabosa, "Electromagnetically induced gratings in a degenerate open two-level system," Phys. Rev. A **65**(3), 033803 (2002).
25. T. Hong, "Spatial weak-light solitons in an electromagnetically induced nonlinear waveguide," Phys. Rev. Lett. **90**(18), 183901 (2003).
26. Y. Zhang, C. Yuan, Y. Zhang, H. Zheng, H. Chen, C. Li, Z. Wang, and M. Xiao, "Surface solitons of four-wave mixing in electromagnetically induced lattice," Laser Phys. Lett. **10**(5), 055406 (2013).
27. U. Khadka, J. Sheng, and M. Xiao, "Spatial domain interactions between ultra-weak optical beams," Phys. Rev. Lett. **111**(22), 223601 (2013).
28. J. Sheng, M.-A. Miri, D. N. Christodoulides, and M. Xiao, "PT-symmetric optical potentials in a coherent atomic medium," Phys. Rev. A **88**(4), 041803 (2013).
29. K. G. Makris, R. El-Ganainy, D. N. Christodoulides, and Z. H. Musslimani, "Beam dynamics in PT symmetric optical lattices," Phys. Rev. Lett. **100**(10), 103904 (2008).
30. A. André and M. D. Lukin, "Manipulating light pulses via dynamically controlled photonic band gap," Phys. Rev. Lett. **89**(14), 143602 (2002).
31. Q. He, Y. Xue, M. Artoni, G. C. La Rocca, J. Xu, and J. Gao, "Coherently induced stop-bands in resonantly absorbing and inhomogeneously broadened doped crystals," Phys. Rev. B **73**(19), 195124 (2006).

## 1. Introduction

Optical waveguide lattices have been a subject of intensive studies recently [1,2]. Such periodic arrays of evanescently coupled optical waveguides exhibit a range of interesting properties which are otherwise unattainable in the bulk. One of the best known examples is the discrete diffraction of light in optical waveguide arrays [2]. Such photonic lattices have been used to directly observe and study optical analogs of many fundamental quantum mechanical effects like Bloch oscillations [3, 4], Zener tunneling [5], quantum random walks [6], and Anderson localization [7] to mention a few. In addition, optically induced photonic waveguide lattices have been also utilized to observe one and two dimensional discrete spatial solitons in photorefractive crystals [8–11].

On the other hand, it has been known that optical wave-guiding effects can be achieved in coherently prepared atomic media with electromagnetically-induced transparency (EIT) [12–14]. In general, EIT makes an absorptive medium transparent to a weak probe field. Such transparency results from the destructive quantum interference induced by a strong coupling field [15,16]. This in turn leads to an enhanced nonlinear susceptibility in the spectral region of the induced transparency and is associated with a steep dispersion [17,18]. In multi-level atomic systems, many intriguing spatial phenomena have been observed in EIT-related systems. These include electromagnetically induced focusing [19], self-imaging [20], electromagnetically induced gratings [21–24], and soliton formation [25–27]. All these interesting observations result from the spatial variation of the refractive index in an EIT or EIT-related atomic medium. In such coherent atomic systems, one can simply control different experimental parameters to get an optimal configuration for desired applications.

In this work, we utilize the EIT effect to spatially modify the refractive index of the Doppler-broadened rubidium atoms. In this manner, we establish an optically induced lattice in the transverse direction, so that discrete diffraction patterns can be formed when a weak probe beam propagates through the induced lattice. We have also observed that the diffraction pattern can be controlled through the atomic parameters such as two-photon detuning and temperature, as well as orientations of the coupling and probe beams. A periodic arrangement of such optical waveguides has not been explored in atomic media to the best of our knowledge. Due to the many available tunable parameters, such multi-level atomic system provides a unique platform to investigate underlying physics for multi-channel lattice

#240649 Received 11 May 2015; revised 25 Jun 2015; accepted 28 Jun 2015; published 22 Jul 2015
© 2015 OSA

potentials for the refractive index, which can be very useful in understanding interesting effects such as PT symmetry optics [28,29] and discrete solitons [10].

## 2. Experimental setup and theory

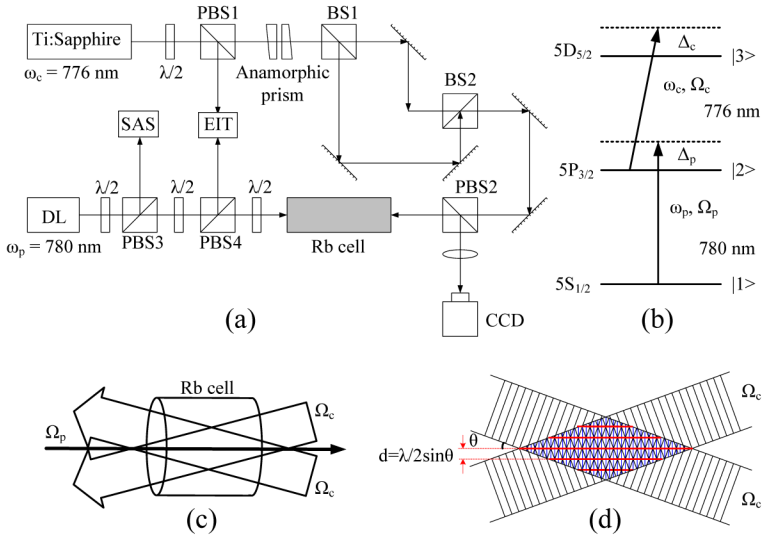


Fig. 1. (a) Experimental setup: PBS, polarization beam splitter; SAS, saturation absorption spectroscopy; EIT, monitoring the two-photon electromagnetically induced transparency condition; λ/2, half-wave plate; (b) The relevant three-level rubidium atomic system; (c) The schematic for generating an optically induced lattice in a hot rubidium vapor cell. (d) Snapshot of the optical lattice in (c).

The experimental setup and the associated atomic energy levels of $^{87}$Rb are shown in Figs. 1(a) and 1(b). The coupling beams are obtained from a Ti:Sapphire ring laser working at 776 nm driving the transition between levels |2> and |3> ($5P_{3/2}\rightarrow5D_{5/2}$). The probe beam on the other hand, comes from a single-mode tunable diode laser (Toptica DL 100) with stabilized current and temperature, operating at the wavelengths of 780 nm and probes the lower transition between levels |1> and |2> ($5S_{1/2}\rightarrow5P_{3/2}$). The coupling and probe lasers are both continuous waves. A polarization beam splitter (PBS1) is used to split the initial coupling beam into two beams. The reflected (vertically-polarized) beam is used as the coupling beam for setting an EIT reference signal. The transmitted beam (horizontally-polarized and nearly circular in shape), is transformed into an elliptical shape by using an anamorphic prism pair. After passing through a beam splitter (BS1), the coupling beam splits into two beams with the same intensities and the same spatial shapes. These two elliptically-shaped coupling beams then recombine at BS2 and propagate toward a 7.5 cm long Rb cell while maintaining an angle of $2\theta \approx 0.4°$ with respect to each other, as shown in Figs. 1(c) and 1(d). As a result of interference between these two coupling beams a standing wave appears in the transverse direction whose period is determined to be $d = \lambda/(2\sin\theta) \approx 112$ μm. It is worth mentioning that a standing wave in the propagating direction with a period of $\lambda/(2\cos\theta)$ is created simultaneously, which is typically associated with the so-called photonic band-gap [30,31]. Since it will affect the transmission/reflection of the probe beam uniformly, and does not lead to the diffraction in the transverse directions, we only consider the lattice in the transverse direction in this work. The Gaussian-shaped probe beam counter-propagates with respect to the two strong coupling beams and overlaps well with the optical lattice induced by these two coupling beams inside the atomic vapor cell. The input probe beam size before cell is ~100 μm. The output of the probe beam is imaged onto a CCD camera with a lens to ensure that the

#240649 Received 11 May 2015; revised 25 Jun 2015; accepted 28 Jun 2015; published 22 Jul 2015
© 2015 OSA

CCD takes the images of the output plane of the cell. The frequency detunings of the probe and coupling fields are $\Delta_p = \omega_p - \omega_{12}$ and $\Delta_c = \omega_c - \omega_{23}$, respectively.

The key ingredient of this experiment is to make a good optically induced lattice so that the probe light can be confined at the discrete sites in the weakly guiding waveguides of the lattice, which means that the contrast of the real part of the refractive index, i.e. the difference of the refractive index at nodes and antinodes of the optically induced lattice, should be large enough to guide the light, while in the mean time the absorption contrast (the imaginary part of the refractive index) should be as small as possible to reduce the effect of the absorption on the output images, and this is the reason why we choose the single photon detuning, i.e. the probe and coupling detunings, to be ~400 MHz. By utilizing the density-matrix method [28], we can obtain the spatially modified refractive index as a function of the transverse coordinate x, which is due to the periodical modulation of the coupling beam intensity from the interference, as shown in Fig. 2. Such modulated index profile clearly indicates a one-dimensional optical lattice.

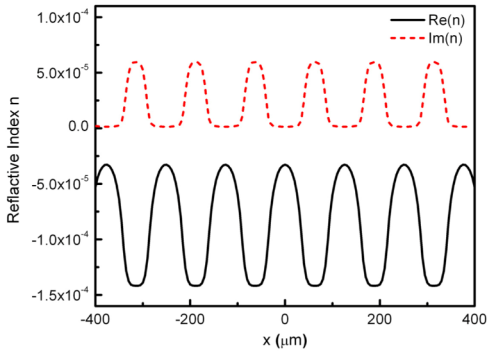


Fig. 2. Numerically calculated plots of the spatially modified real (solid line) and imaginary (dashed line) parts of the refractive index modulation, respectively. Here, $\Delta_c = -400$ MHz, $\Delta_p = 390$ MHz, and $\Omega_c = 200\cos^2(x/40)$.

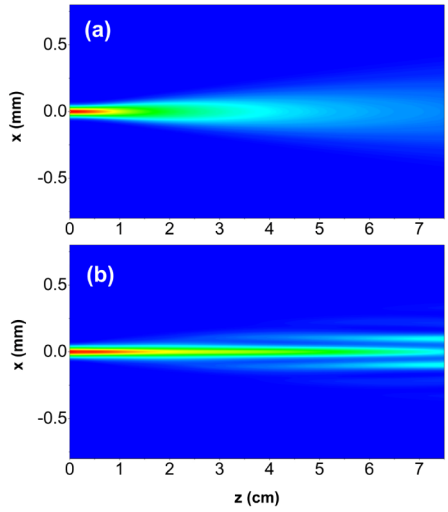


Fig. 3. Theoretical simulations of the probe beam propagation. (a) Normal diffraction of a Gaussian beam without the coupling beam; (b) Evolved discrete diffraction of the weak Gaussian beam in an optical lattice.

The diffraction pattern of a weak probe Gaussian beam propagating in such an optical lattice can be numerically simulated by using beam propagation method [29], as presented in

#240649 Received 11 May 2015; revised 25 Jun 2015; accepted 28 Jun 2015; published 22 Jul 2015
© 2015 OSA

Fig. 3. The parameters used in this simulation are as follows: the lattice space is ~126 μm, the complex refractive index is $n = n_0 + (10^{-5} + 0.5\times10^{-5} i)\cos(x/x_0)$. Here $n_0$ = 1 is the background index of the atomic medium and $x_0$ = 20 μm is a scale factor. In the absence of the coupling beams, the output of the probe field through the Rb cell still maintains a Gaussian shape with normal diffraction, as shown in Fig. 3(a). However, when the optically induced lattice is introduced (in the presence of the interfering coupling beams), the discrete diffraction occurs as depicted in Fig. 3(b), which has a dramatically changed output profile as compared to that of Fig. 3(a).

## 3. Experimental results and discussion

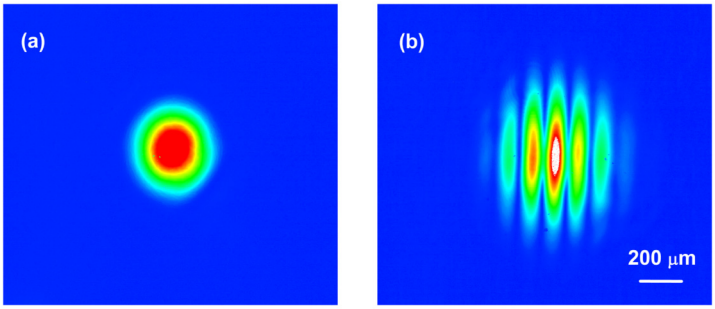


Fig. 4. Experimental results of the probe beam's output intensity images. (a) Output of a Gaussian probe beam propagating through the cell with the coupling beams blocked. (b) Output of a Gaussian probe beam after propagating through an optical lattice.

The experimentally measured output intensities of the probe beam are displayed in Fig. 4 for the two cases, i.e. without and with the optically induced lattice. As shown in Fig. 4(a), in the absence of the coupling beams, the output of the probe beam still remains Gaussian, since only normal diffraction occurs when the probe light passes through the cell, whereas, as shown in Fig. 4 (b), when the coupling beams are present, the output of the probe beam appears stripe pattern, this is because discrete diffraction happens when the probe beam passes through the optical lattice, which has been predicted in Fig. 3(b). The distance between the adjacent bright channels in Fig. 4(b) is the same as the separation of the waveguides in the optical lattice. The power of each coupling beam and the probe beam are 17.0 mW and 1.5 mW, respectively.

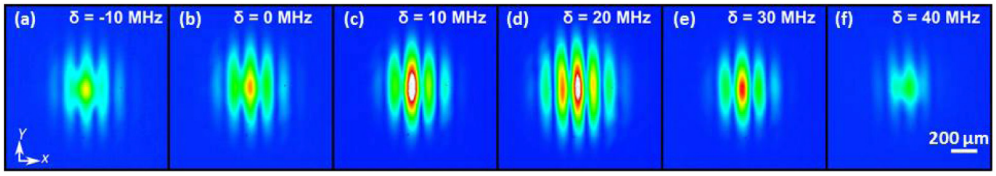


Fig. 5. Experimentally observed diffraction patterns of the probe beam propagating through the optical lattice, as the two-photon detuning δ is changed. (a) δ = –10, (b) δ = 0, (c) δ = 10, (d) δ = 20, (e) δ = 30, and (f) δ = 40 MHz, respectively.

The diffraction pattern is sensitive to several experimental parameters. The first one is lattice constant, which is determined by the angle between the two coupling beams. After the frequency detunings of both the coupling and probe fields are set, we need to carefully adjust the lattice spacing to match the optimal refractive index in order to enhance the contrast of the diffraction pattern. Another parameter is the temperature of the vapor cell. The refractive index obeys $n \sim \frac{N\mu_{12}}{\varepsilon_0 E_p}\mathrm{Re}(\rho_{21})$ [28], where $\mu_{12}$ represents the dipole moment between state |2> and |1>, and N is the atomic density. Increasing the temperature of the Rb cell increases

#240649 Received 11 May 2015; revised 25 Jun 2015; accepted 28 Jun 2015; published 22 Jul 2015
© 2015 OSA

the density of Rb atoms, which gives a larger refractive index contrast. In our experiment, the temperature is kept at about 100 °C (the corresponding atomic density and Doppler width are ~$6*10^{12}$ $cm^{-3}$ and 570 MHz, respectively), and the refractive index contrast is estimated to be $10^{-5}$. The third parameter is the relative position between the incident probe beam and the induced optical lattice. The input probe beam can be either centered between two maxima or on top of one maximum. Changing the relative input position in the transverse direction will significantly alter the diffraction pattern. In our experiment, the probe beam is centered on one maximum of the induced lattice, i.e. the center of one waveguide. The output image has the brightest strip in the center, and the intensities of strips on both sides will gradually decrease but still be symmetric. The fourth parameter is the two-photon frequency detuning $\delta = \Delta_c + \Delta_p$. The diffraction pattern is very sensitively dependent on δ. We can only find discrete diffraction patterns within a frequency detuning window of ~60 MHz near the two-photon (EIT) resonance, as shown in Fig. 5. When δ is about 20 MHz, the most clear and brightest diffraction pattern is obtained as shown in Fig. 5(d). This is because the real part of the refractive index has better shape at delta = 20MHz than at delta = 0, which is more favorable to guide light in each channel. As δ shifts away from the optimal point of 20 MHz, the contrast of diffraction pattern for the observable discrete spots drops significantly. In Figs. 4 and 5, the white areas present the highest intensity and the blue areas have the lowest intensity. It is worth mentioning that the diffraction patterns in Figs. 4 and 5 are the images on the output plane of the cell, therefore, they are quite different from the Fraunhofer diffraction from electromagnetically induced grating as proposed in [21], Ling et al. Also, in principle, it is possible to observe the discrete diffraction pattern as predicted in Fig. 3(b) from the side view of the cell [27].

## 4. Conclusion

In conclusion, we have experimentally observed discrete diffraction patterns in an optically induced lattice created by interferring two strong coupling beams in a three-level rubidium atomic system inside a vapor cell. The change of the diffraction pattern under different two-photon frequency detunings has been experimentally invesitigated. In addition, theoretical simulation has been performed to better understand such discrete diffraction phenomenon in optical lattices. Since optically induced lattices in coherently prepared atomic media offer a wide range of controlling parameters, the demonstrated results can provide a versatile platform and a novel way in experimentally studying optical lattices. Given that gain/loss and nonlinearity can also be incorporated in such systems, EIT-induced optical lattices can also be utilized to investigate optical solitons as well as PT-symmetry related phenomena [28].

#240649 Received 11 May 2015; revised 25 Jun 2015; accepted 28 Jun 2015; published 22 Jul 2015
© 2015 OSA